

# Quantifying Infrastructure Resilience to Land Subsidence Hazards in Alaska by Leveraging Spaceborne InSAR Measurements and Mapping

Jonathan Lucy<sup>1,2</sup>, Manoochehr Shirzaei<sup>1,2</sup>, Susanna Werth<sup>1,2</sup>

<sup>1</sup> Virginia Tech, Geosciences, <sup>2</sup> UNU Institute for Water, Environment, and Health

## Abstract

Arctic regions are experiencing rapid warming, accelerating permafrost degradation, and increasing land subsidence, all of which threaten critical infrastructure. This study presents a framework for infrastructure risk assessment by leveraging spaceborne Interferometric Synthetic Aperture Radar (InSAR) to quantify vertical land motion (VLM) and differential settlement across Alaska. By using Sentinel-1 C-band SAR images from 2016-2024, deformation time series were generated at ~40 m spatial resolution and paired with geospatial datasets of urban areas and transportation networks. To better capture subsidence-related hazards, a distortion-angle metric was used to quantify spatial variability in deformation. Results in this study indicate widespread subsidence in cities such as College, Alaska, with a median VLM rate of -4.5 mm/yr within the city boundary, and Anchorage showing high rates of differential settlement. In addition, our results reveal that more than 55% of the transportation infrastructure examined in this study is experiencing subsiding deformation. This work highlights the potential for missions such as NISAR to enhance infrastructure risk detection and more robust infrastructure resilience planning in Arctic environments.

## Introduction

Arctic regions are among the fastest-warming areas on the globe, with temperatures rising four times faster than the global average<sup>1</sup>. The warming climate has caused much of the ice-rich permafrost, or perennially frozen ground, to melt and degrade<sup>2</sup>. This degradation of permafrost results in a decrease in the load-bearing capacity of the soil, leading to land subsidence, or downward movement of the ground<sup>3,4</sup>. Increased land subsidence holds implications for infrastructure, such as damage,

impairment, and disruption<sup>4,5</sup>. These impacts of land subsidence are intensified in Arctic regions, such as Alaska, where many isolated communities rely on fragile transportation networks for safe travel and access to supplies<sup>6</sup>.

To ensure Alaskan current and future infrastructure remains resilient in the face of a warming climate, infrastructure managers and planners must have strategies in place to adapt to the changing landscape<sup>7,8</sup>. With \$276 billion in infrastructure projected to be affected by warming temperatures and \$1 trillion in future investments expected in the region, it is imperative that large-scale monitoring efforts and adaptation strategies are in place to

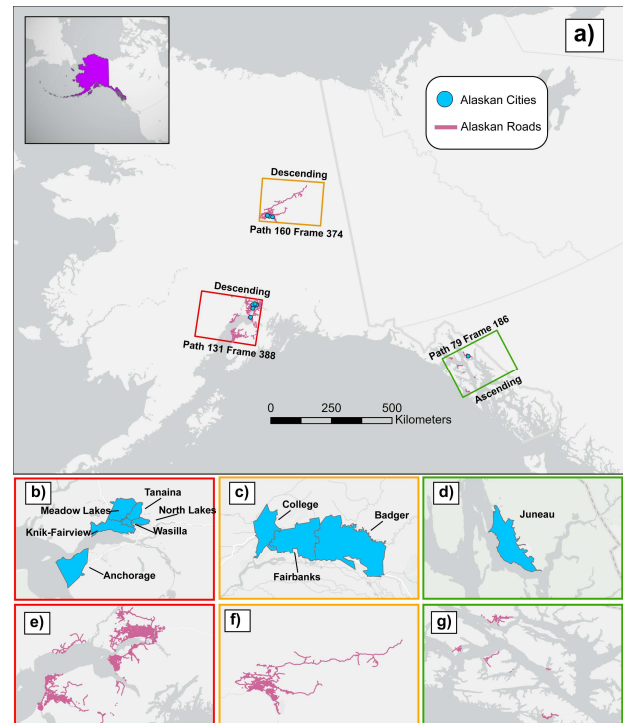


Figure 1: Locator map of Sentinel-1 frame coverage of Alaskan cities and routes. The frame color in map (a) corresponds to panels (b) – (g). Pannels (b) – (d) illustrate city boundaries within frames, while panels (e) - (g) show AKDOT routes within frames

improve the resilience of current and future Alaskan infrastructure<sup>9,10</sup>.

While valuable in-situ deformation-monitoring technologies exist, such as GNSS, these stations can be spaced far apart, particularly in Alaska. This sparse distribution of stations can lead to coarse resolution deformation mapping. To supplement these in-situ stations, radar-equipped satellites have been launched to monitor land deformation from space.

To this end, this study aims to harness the capabilities of spaceborne Interferometric Synthetic Aperture Radar (InSAR) to capture large-scale deformation with high precision and accuracy, thereby identifying areas where infrastructure is exposed to land deformation hazards. This work is intended to provide additional information to state and federal asset managers to make more informed decisions about future mitigation and monitoring strategies.

### Data & Methods

VLM data over Alaskan cities and transportation infrastructure was generated by leveraging the WabInSAR software alongside Sentinel-1 C-band Single Look Complex (SLC) images<sup>11-15</sup> downloaded from the Alaska Satellite Foundation (ASF). The processed deformation data includes 3 Sentinel-1 frames and 556 images, spanning 2016 – 2024. The final spatial resolution of the deformation pixels is  $\sim 40$  meters, and the time series interval is 12 days. The deformation results are then referenced to a GPS station near the city, so the velocities are representative of deformation occurring in the area. Once the VLM data were generated, shapefiles of Alaskan city boundaries and transportation infrastructure were overlaid to select pixels that intersect the city boundaries and transportation features. This ensures an accurate representation of the infrastructure's deformation (Figure 2). Since our satellite observations provide only one viewing angle per orbit, to project our line-of-sight (LOS) velocities into the vertical direction, we divide the velocity results by the cosine of the incidence angle.

While subsidence can cause multiple hazards, one major hazard driven by subsidence is differential settlement, in which the ground deforms unevenly. This poses threats to infrastructure and can result in structural damage to buildings and infrastructure<sup>16-19</sup>. To quantify differential

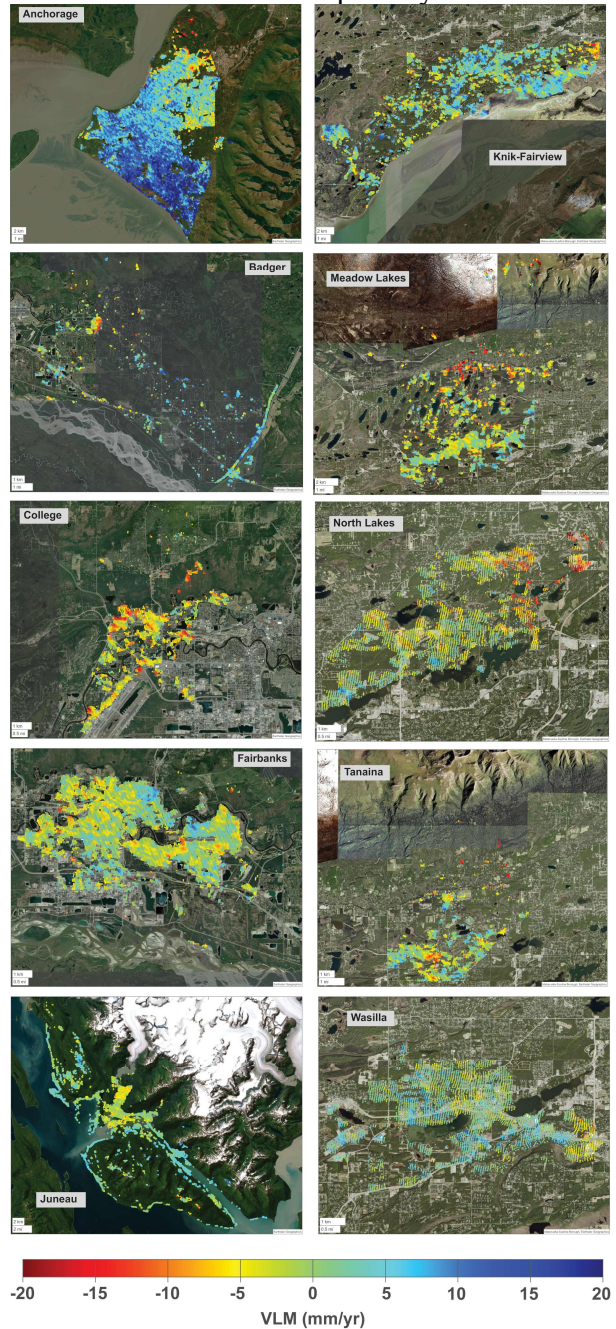


Figure 2: Maps depicting the spatial distribution of deformation pixels over each city in the study. Each map is labeled with the city name, with warmer-color pixels representing subsidence and cooler-colored pixels representing uplift.

settlement, this study uses a distortion angle calculation, where  $\beta$  is the distortion angle measurement,  $\delta$  is the difference in vertical displacement between the two pixels, and  $l$  is the horizontal distance between them:

$$\beta = \frac{\delta}{l} \quad (1)$$

The city selection was based on population data from the U.S. Census Bureau<sup>20</sup>, with the top 10 cities with the highest populations chosen. The city boundaries used in this study were sourced from the U.S. Census Bureau. The Juneau boundary shapefile was edited to primarily cover the city's metropolitan area, because a large portion of its boundary lies within densely forested regions. Transportation shapefiles were selected from the Alaska Department of Transportation and Public Facilities (AKDOT&PF) data repository. Since these are linear features, a 100-meter buffer was added to all transportation features to ensure adequate pixel extraction<sup>21</sup>.

## Results

### VLM

Once cities were identified by population size, pixels intersecting the city boundaries were extracted. The cities chosen for this study included Anchorage, Badger, College, Knik-Fairview, Meadow Lakes, North Lakes, Tanaina, and Wasilla. After selecting pixels over city boundaries, the total pixel count across the ten cities reached 87,424. We observe a range of VLM rates, with the fastest median subsidence rates occurring in College, at  $4.5 \text{ mm/yr} \pm 0.8 \text{ mm/yr}$ . Hotspots of subsidence within College are located to the north of Fairbanks International Airport and directly west of the University of Alaska, Fairbanks. The city with the fastest uplift rates was Anchorage, with a median VLM rate of  $8.0 \text{ mm/yr} \pm 1.0 \text{ mm/yr}$ . A majority of the uplift observed in Anchorage is to the south and west of the city.

Transportation networks included in this study were Alaska Department of Transportation (AKDOT) routes residing in the

three frames processed. Of the three frames, a total of 100,488 pixels intersected AKDOT

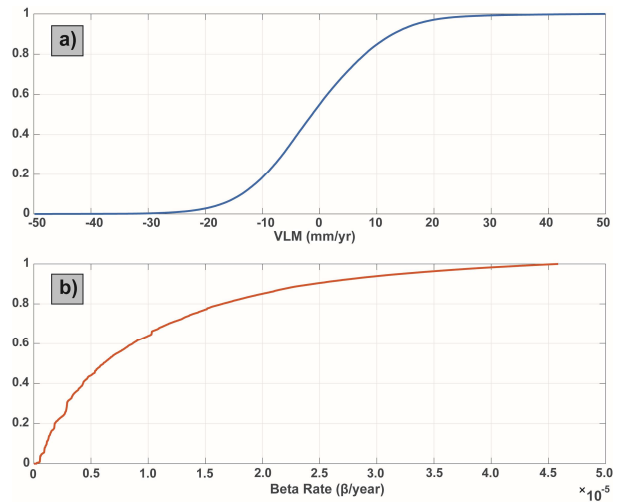


Figure 4: Plots showing CDFs of VLM rates (a) and beta rates (b) over AKDOT routes

routes. Of all deformation observed over AKDOT routes, 55.1% was subsiding deformation with a median VLM rate of  $-1.3 \text{ mm/yr} \pm 0.2 \text{ mm/yr}$ .

### Distortion Angle

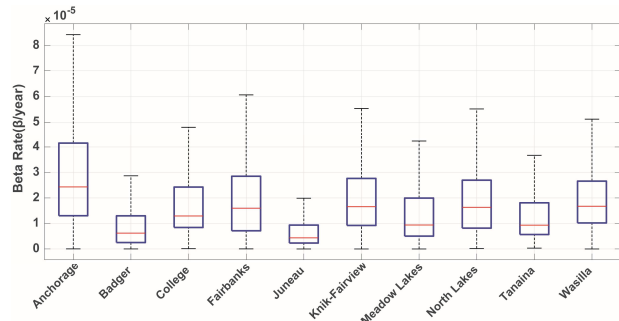


Figure 3: Box plots showing distribution of distortion angle measurements for each city

To quantify hazards related to land deformation, differential settlement was calculated using the distortion angle calculation (Equation 1) across all infrastructure in the study. Of the 10 cities, Anchorage showed the fastest median rate of distortion angle, at  $2.43 \times 10^{-5}$  per year. Hot spots of differential settlement in Anchorage are concentrated along the southern coast and near the Potter Marsh Watershed Park. The same procedure was applied to the transportation sector. This infrastructure sector

in Alaska is experiencing median rates of differential settlement at  $6.9 \times 10^{-6}$  /yr, with hotspots appearing to the northeast of Fairbanks on the Steese Highway.

### Discussion

#### Next Steps

The next steps in this work include translating the observed distortion angle rates into cumulative distortion angle to better capture infrastructure stress over time. This will be achieved by multiplying the total observation period by the InSAR derived distortion angle rate. The values will then be grouped using published thresholds from literature. This classification will enable straightforward identification of locations with increased infrastructure risk and actionable guidance for asset managers.

#### Implications for Infrastructure Assets

The results of this study demonstrate the utility of spaceborne InSAR as a scalable tool for identifying regions and infrastructure exposed to land deformation hazards across large, remote regions. Leveraging VLM measurements alongside infrastructure features, this approach enables a systematic screening of assets that may be susceptible to differential settlement. Spaceborne InSAR fills the gap of in-situ monitoring networks, which are often very sparse, especially in Arctic regions such as Alaska.

The use of the distortion angle as a proxy for differential settlement adds to the applicability of infrastructure assessment. While VLM rates alone describe the magnitude of ground motion, the distortion angle captures spatial variability in ground deformation, which is linked to structure variables such as stress. The identification of differential settlement rates in areas such as the southern coast of Anchorage, as well as transportation corridors along the Steese Highway northeast of Fairbanks, suggests these locations may warrant prioritized monitoring.

From an asset management perspective, geospatial analysis can support agencies such as AKDOT&PF in allocating limited resources more effectively. With extensive infrastructure networks distributed across the state, decision-

makers require tools to identify potential risk hotspots in difficult terrain. The methodology presented here allows for a data-driven approach to inform maintenance prioritization, guide field investigations, and support long-term resilience planning.

#### NISAR

This study underscores the growing role of satellite remote sensing in assessing infrastructure resilience challenges. In areas with sparse data coverage like Alaska, leveraging C-band SAR images from Sentinel-1 demonstrates the feasibility of large-scale deformation monitoring at high spatial and temporal resolution. With the launch of the NASA-ISRO Synthetic Aperture Radar (NISAR) mission, it is expected that future InSAR derived deformation studies can leverage this new satellite. NISAR's L-band images will offer improved coherence over vegetated areas, addressing a key limitation of C-band systems. Additionally, the provided global coverage will allow for consistent image acquisitions and time steps.

#### Limitations

Several limitations should be considered when interpreting the results presented in this study. First, the use of C-band introduces sensitivity to vegetation cover, reducing coherence and overall pixel coverage. This is apparent in metropolitan areas with vegetated areas, which exhibit low pixel densities.

Second, not all infrastructure included in this study is underlain by permafrost. As a result, permafrost degradation cannot be labeled as a driver of land deformation for all infrastructure in this study. This is mainly relevant for infrastructure in the southern portion of the state.

Third, the projection of line-of-sight (LOS) measurement into the vertical direction assumes that all deformation is vertical. In reality, ground deformation can include a horizontal component, which is not accounted for.

Finally, the absence of in-situ validation limits the ability to quantitatively assess the accuracy of the InSAR derived deformation. While results are referenced to a GPS station,

future results should be validated with additional GPS stations when available.

### Conclusion

This study demonstrates the potential of spaceborne InSAR to support large-scale infrastructure hazard assessment in Arctic environments. By integrating deformation measurements with infrastructure datasets, this work presents a framework capable of identifying areas where assets may be exposed to land subsidence and differential settlement. Further advancements in satellite remote sensing, particularly through missions such as NISAR, are expected to improve this approach by adding globally available L-band images. Continued integration of remote sensing data and ground-based observations alongside geotechnical information will be essential in advancing infrastructure resilience in changing Arctic regions

### References

1. Rantanen, M. *et al.* The Arctic has warmed nearly four times faster than the globe since 1979. *Commun Earth Environ* **3**, 1–10 (2022).
2. Hjort, J. *et al.* Degrading permafrost puts Arctic infrastructure at risk by mid-century. *Nat Commun* **9**, 5147 (2018).
3. Nelson, F. E., Anisimov, O. A. & Shiklomanov, N. I. Subsidence risk from thawing permafrost. *Nature* **410**, 889–890 (2001).
4. Bommer, C., Phillips, M. & Arenson, L. U. Practical recommendations for planning, constructing and maintaining infrastructure in mountain permafrost. *Permafrost and Periglacial Processes* **21**, 97–104 (2010).
5. Hjort, J. *et al.* Impacts of permafrost degradation on infrastructure. *Nat Rev Earth Environ* **3**, 24–38 (2022).
6. Ford, J. D., Bell, T. & St-Hilaire-Gravel, D. Vulnerability of Community Infrastructure to Climate Change in Nunavut: A Case Study From Arctic Bay. in *Community Adaptation and Vulnerability in Arctic Regions* (eds Hovelsrud, G. K. & Smit, B.) 107–130 (Springer Netherlands, Dordrecht, 2010). doi:10.1007/978-90-481-9174-1\_5.
7. *Arctic Climate Impact Assessment*. (Cambridge University Press, Cambridge ; New York, N.Y, 2005).
8. *Snow, Water, Ice and Permafrost in the Arctic (SWIPA): Climate Change and the Cryosphere*. (AMAP, Oslo, Norway, 2011).
9. Atkisson, A. A wave of investment. *The Circle* **16** (2018).
10. Streletskiy, D. A., Clemens, S., Lanckman, J.-P. & Shiklomanov, N. I. The costs of Arctic infrastructure damages due to permafrost degradation. *Environ. Res. Lett.* **18**, 015006 (2023).
11. Shirzaei, M. & Walter, T. R. Estimating the Effect of Satellite Orbital Error Using Wavelet-Based Robust Regression Applied to InSAR Deformation Data. *IEEE Trans. Geosci. Remote Sensing* **49**, 4600–4605 (2011).
12. Shirzaei, M. A Wavelet-Based Multitemporal DInSAR Algorithm for Monitoring Ground Surface Motion. *IEEE Geoscience and Remote Sensing Letters* **10**, 456–460 (2013).
13. Shirzaei, M. A seamless multitrack multitemporal InSAR algorithm. *Geochemistry, Geophysics, Geosystems* **16**, 1656–1669 (2015).
14. Shirzaei, M., Bürgmann, R. & Fielding, E. J. Applicability of Sentinel-1 Terrain Observation by Progressive Scans multitemporal interferometry for monitoring slow ground motions in the San Francisco Bay Area. *Geophysical Research Letters* **44**, 2733–2742 (2017).
15. Lee, J.-C. & Shirzaei, M. Novel algorithms for pair and pixel selection and atmospheric error correction in multitemporal InSAR. *Remote Sensing of Environment* **286**, 113447 (2023).
16. Fernández-Torres, E., Cabral-Cano, E., Solano-Rojas, D., Havazli, E. & Salazar-Tlaczani, L. Land Subsidence risk maps and InSAR based angular distortion structural

vulnerability assessment: an example in Mexico City. *Proc. IAHS* **382**, 583–587 (2020).

17. Cigna, F. & Tapete, D. Present-day land subsidence rates, surface faulting hazard and risk in Mexico City with 2014–2020 Sentinel-1 IW InSAR. *Remote Sensing of Environment* **253**, 112161 (2021).
18. Vassileva, M. *et al.* A decade-long silent ground subsidence hazard culminating in a metropolitan disaster in Maceió, Brazil. *Scientific Reports* **11**, 7704 (2021).
19. Ohenhen, L. O. & Shirzaei, M. Land Subsidence Hazard and Building Collapse Risk in the Coastal City of Lagos, West Africa. *Earth's Future* **10**, e2022EF003219 (2022).
20. U.S. Census Bureau, U. S. D. of C. Age and Sex.
21. Alaska Department of Transportation and Public Facilities. Alaska Critical Infrastructure.